

## Loss of CARM1 Results in Hypomethylation of Thymocyte Cyclic AMP-regulated Phosphoprotein and Deregulated Early T Cell Development\*

Received for publication, March 5, 2004, and in revised form, April 12, 2004  
Published, JBC Papers in Press, April 19, 2004, DOI 10.1074/jbc.M402544200

Jeesun Kim‡, Jaeho Lee‡, Neelu Yadav‡, Qi Wu‡, Carla Carter‡, Stéphane Richard§, Ellen Richie‡, and Mark T. Bedford‡¶

From the ‡The University of Texas M. D. Anderson Cancer Center, Science Park-Research Division, Smithville, Texas 78957 and §Lady Davis Institute for Medical Research, McGill University, Montréal, Québec H3T 1E2, Canada

**The coactivator-associated arginine methyltransferase, CARM1, is a positive regulator of transcription. Using high density protein arrays, we have previously identified *in vitro* substrates for CARM1. One of these substrates, TARPP (thymocyte cyclic AMP-regulated phosphoprotein), is expressed specifically in immature thymocytes. Here, we have demonstrated that TARPP is arginine-methylated at a single residue, Arg<sup>650</sup>, both *in vitro* and *in vivo*. In addition, recombinant TARPP is not methylated by extracts from *Carm1*<sup>-/-</sup> cells, indicating that there is no redundancy in this pathway. We show that thymi from *Carm1*<sup>-/-</sup> embryos (E18.5) have a 5–10-fold reduction in cellularity compared with wild type littermates. Flow cytometric analysis of thymocytes revealed a decrease in the relative proportion of double negative thymocytes in *Carm1*<sup>-/-</sup> embryos because of a partial developmental arrest in the earliest thymocyte progenitor subset. These results demonstrate that CARM1 plays a significant role in promoting the differentiation of early thymocyte progenitors, possibly through its direct action on TARPP.**

Arginine methylation is a common posttranslational modification that can regulate protein function (1, 2). The main pool of proteins that are arginine-methylated possess RNA binding properties (3). In addition, enzymes that facilitate histone acetylation (CBP<sup>1</sup>/p300), and histones are themselves arginine-methylated, thus implicating this posttranslational modification in chromatin remodeling and transcriptional regulation

(4–7). The methylation of arginine residues is catalyzed by at least two different classes of protein arginine methyltransferase (PRMT) enzymes (3). The Type I enzymes catalyze the formation of asymmetric N<sup>G</sup>,N<sup>G</sup>-dimethylarginine residues, and the Type II enzyme catalyzes the formation of symmetric N<sup>G</sup>,N<sup>G</sup>-dimethylarginine residues. Both enzyme types generate N<sup>G</sup>-monomethylarginine (MMA) intermediates. The cloning of the yeast Type I arginine methyltransferase enzyme (8, 9) Hmt1p (also known as Rmt1p) provided the molecular framework for the identification of six homologs in mammals (PRMT1–6). Currently, known mammalian Type I enzymes include PRMT1 (10, 11), the zinc finger-containing enzyme PRMT3 (12), the coactivator-associated arginine methyltransferase PRMT4/CARM1 (4), and the nuclear enzyme PRMT6 (13). The only mammalian Type II PRMT identified to date is the Janus kinase-binding protein JBPI/PRMT5 (14, 15). Activity for the SH3 domain-containing arginine methyltransferase PRMT2 has yet to be clearly demonstrated.

The coactivator-associated arginine methyltransferase (CARM1/PRMT4) is an enzyme that catalyzes the formation of asymmetric N<sup>G</sup>,N<sup>G</sup>-dimethylarginine residues (5). CARM1 was identified as a binding partner for the p160 family of nuclear hormone receptor coactivators (4). The recruitment of CARM1 enhances transcriptional activation by nuclear receptors, possibly as a result of the specific methylation of histone H3 and/or CBP/p300. Further attempts to elucidate the biological role of CARM1 have included the targeted disruption of the *Carm1* genes in mice and the search for *in vivo* substrates for this enzyme (16, 17).

PRMTs target a wide array of different proteins for posttranslational modification. The majority of asymmetric N<sup>G</sup>,N<sup>G</sup>-dimethylarginine residues occur within glycine- and arginine-rich (GAR) domains (3). Proteins with methylated GAR domains include Sam68, heterogeneous nuclear ribonucleoprotein K, heterogeneous nuclear ribonucleoprotein U, ILF3, and FUS (16, 18). CARM1 displays a higher degree of specificity than other Type I enzymes and does not methylate GAR domains (16). CARM1 substrates have been identified through candidate approaches (histone H3 and Hu antigen R) (4, 19), through serendipitous discovery (CBP/p300) (6), and through focused *in vitro* substrate screens (PABP1 and TARPP) (16). Here we have demonstrated that the early T cell-specific factor TARPP (thymocyte cyclic AMP-regulated phosphoprotein) (20), which was identified as a CARM1 substrate using high density protein arrays, is methylated *in vivo*. We went on to map the single arginine residue that is targeted for posttranslational modification by CARM1. Finally, we have shown that T cell development in *Carm1* mutant embryos (E18.5) is aberrant, concomitant with the start of TARPP expression.

\* The costs of publication of this article were defrayed in part by the payment of page charges. This article must therefore be hereby marked "advertisement" in accordance with 18 U.S.C. Section 1734 solely to indicate this fact.

¶ Supported by National Institutes of Health Grant DK62248–01 and, in part, by institutional grants from the National Institutes of Health (CA16672) and NIEHS, National Institutes of Health (ES07784). To whom correspondence should be addressed. Tel.: 512-237-9539; Fax: 512-237-2475; E-mail: mtbedford@mdanderson.org.

<sup>1</sup> The abbreviations and trivial terms used are: CBP, CREB (cAMP-response element-binding protein)-binding protein; PRMT, protein arginine N-methyltransferase; [<sup>3</sup>H]AdoMet, S-adenosyl-L-[methyl-<sup>3</sup>H]methionine; MMA, ω-N<sup>G</sup>-monomethylarginine; TARPP, thymocyte cyclic AMP-regulated phosphoprotein; PABP1, poly(A)-binding protein 1; CARM1, coactivator-associated arginine methyltransferase 1; GST, glutathione S-transferase; GST-GAR, GST fusion protein containing the glycine- and arginine-rich N-terminal region of fibrillarlin; GFP, green fluorescent protein; PBS, phosphate-buffered saline; DN, double negative; R3H, a motif with an invariant arginine residue and a highly conserved histidine residue that are separated by three residues; Sam68, Src-associated substrate during mitosis 68 kDa; MEF, mouse embryonic fibroblast; TCR, T cell receptor; RAG, recombination activat-

## EXPERIMENTAL PROCEDURES

**Antibodies and Plasmids**—pGEX-CARM1 was a gift from Michael Stallcup at the University of Southern California (4). pGEX-GAR was a gift from Steve Clarke at UCLA (3). The generation of pGEX-PABP1 has been described previously (16). All TARPP-GST fusion proteins were subcloned in pGEX6P-1 (Amersham Biosciences). For GFP fusion constructs, pGEX6P-1 fusion constructs were cut and directly subcloned into pEGFP-C1 (Clontech). Site-directed mutagenesis was performed on full-length TARPP in pEGFP-C1 by PCR using mutant primer sets. The  $\alpha$ TARPP antibody was raised in rabbits against GST-TARPPd, which encodes amino acids 622–807 of TARPP (see Fig. 1A). The  $\alpha$ CARM1 antibody was raised in rabbits against the peptide sequence KTMGGPAISMASPMSIPTNTMTHYGS. Other antibodies were purchased from Clontech ( $\alpha$ GFP) and BD PharMingen ( $\alpha$ CD4,  $\alpha$ CD8,  $\alpha$ CD3,  $\alpha$ B220,  $\alpha$ CD11b,  $\alpha$ Gr-1,  $\alpha$ CD44, and  $\alpha$ CD25).

**Preparation of the GST Fusion Protein**—GST fusion proteins were overexpressed in *Escherichia coli* DH5 $\alpha$  cells (Invitrogen) by induction with a final concentration of 0.4 mM isopropyl- $\beta$ -D-thiogalactopyranoside. Washed cells were resuspended in 2 ml of phosphate-buffered saline (PBS; 137 mM NaCl, 2.7 mM KCl, 4.3 mM Na<sub>2</sub>HPO<sub>4</sub>, 1.4 mM KH<sub>2</sub>PO<sub>4</sub>, pH 7.4) and 100  $\mu$ M phenylmethylsulfonyl fluoride/g of cells and subsequently broken by four 30-s sonicator pulses (50% duty; setting “4”) on ice with a Sonifier cell disruptor W-350 (SmithKline Corp.). The resulting lysate was centrifuged for 10 min at 23,000  $\times$  g at 4 °C. The GST fusion protein was then batch-purified from extracts by binding to glutathione-Sepharose 4B beads (Amersham Biosciences) and washed in PBS according to the manufacturer’s instructions in the presence of 100  $\mu$ M phenylmethylsulfonyl fluoride. The purified proteins were eluted from the beads with 30 mM glutathione, 50 mM Tris-HCl, pH 7.5, 120 mM NaCl.

**In Vitro Methylation Assay**—*In vitro* methylation reactions were performed in a final volume of 30  $\mu$ l of PBS (pH 7.4). The reaction contained 0.5–1  $\mu$ g of substrate and 1  $\mu$ g of recombinant CARM1. All methylation reactions were carried out in the presence of 0.42  $\mu$ M [<sup>3</sup>H]AdoMet (79 Ci/mmol from a 12.6- $\mu$ M stock solution; Amersham Biosciences). The reaction was incubated at 30 °C for 1 h and then subjected to fluorography by separation on a 10% SDS-PAGE, transfer to a polyvinylidene difluoride membrane, treatment with Enhance<sup>TM</sup> (PerkinElmer Life Sciences), and exposure to film overnight.

**In Vitro Methylation Assay with Cell Lines**—Mouse embryonic fibroblast lines (MEFs) were grown to 80% confluency on a 10-cm plate. Cells were washed with PBS and scraped off the plate into 500  $\mu$ l of PBS (pH 7.4). Cells were lysed by sonication, and the supernatant was used as the enzyme source. *In vitro* methylation reactions were performed by adding the cell lysate to 1  $\mu$ g of GST fusion protein bound to glutathione beads in the presence of 0.42  $\mu$ M [<sup>3</sup>H]AdoMet. The reaction was incubated at 30 °C for 1 h, and then the beads were washed three times with PBS. The substrate-bound beads were then subjected to fluorography for 20 days after SDS-PAGE, transferred to polyvinylidene difluoride membrane, and treated with Enhance<sup>TM</sup>.

**Transient Transfection and in Vivo Methylation Assay**—Cells were labeled using a previously described *in vivo* methylation assay (21). Briefly, for analysis of *in vivo* methylation of TARPP in HeLa cells, GFP fusion constructs were transiently transfected into cells using 30  $\mu$ l of LipofectAMINE 2000 (Invitrogen) in serum-free Dulbecco’s modified Eagle’s medium containing non-essential amino acid solution. One day after transfection, cells were rinsed with PBS to remove serum and then incubated with 5 ml of Met-free Dulbecco’s modified Eagle’s medium containing 10% dialyzed fetal bovine serum, 10  $\mu$ Ci/ml L-[methyl-<sup>3</sup>H]methionine, 100  $\mu$ g/ml cycloheximide, and 40  $\mu$ g/ml chloramphenicol for 3 h. Cells were then lysed in a “mild” buffer (150 mM NaCl, 5 mM EDTA, 1% Triton X-100, 10 mM Tris-HCl, pH 7.5), and immunoprecipitations were performed with  $\alpha$ GFP,  $\alpha$ Sam68, or  $\alpha$ TARPP antibodies. Immunoprecipitates were analyzed by autoradiography after SDS-PAGE and transferred to polyvinylidene difluoride membrane. To gauge the expression levels of GFP-fused proteins, Western blot with an  $\alpha$ GFP antibody was performed using the same membrane.

**Cells**—The generation of wild type and *Carm1*<sup>-/-</sup> MEFs from E13.5 embryos has been described (17). HeLa cells and the BW5147 T cell lymphoma (mature) were obtained from the American Type Culture Collection. The immature T cell lymphoma, LR1–9531, was derived from an *atm*<sup>-/-</sup>*rag-2*<sup>-/-</sup> thymoma and has been described (22). The LR1–9531 cell line was a gift from Boris Reizis at Columbia University.

**Flow Cytometry**—For three-color immunofluorescence analysis, cells in Hank’s balanced salt solution containing 1% bovine serum albumin and 0.1% sodium azide were incubated with directly conjugated or biotinylated Abs on ice for 30 min followed by three washes. Binding of

biotinylated Ab was detected with streptavidin conjugated to allophycocyanin. The cells were fixed in 1% paraformaldehyde before analysis. For determination of double negative (DN) subsets, lineage-positive cells were gated out after staining with a mixture of biotinylated Abs to lineage markers CD4, CD8, CD3, B220, CD11b, and Gr-1 as well as with anti-CD44-phycoerythrin and anti-CD25-fluorescein isothiocyanate (BD PharMingen). Cells were analyzed with a Coulter Epics Elite flow cytometer and analyzed using Coulter Elite software.

## RESULTS AND DISCUSSION

**Mapping of the Methylated Site in TARPP**—Using an arrayed protein library (23), we screened 37,200 clones of His-tagged fusion protein for substrates of the CARM1 arginine methyltransferase. In this manner we identified PABP1 and TARPP as *in vitro* substrates for CARM1 (16). It has since been established that PABP1 is methylated by CARM1 *in vivo* (17). To determine the region of TARPP methylation by CARM1, we generated a contiguous set of GST-TARPP fusion constructs (Fig. 1A). For *in vitro* methylation, GST fusion proteins containing the sequences depicted in Fig. 1A were incubated with recombinant CARM1 in the presence of [<sup>3</sup>H]AdoMet. The C-terminal-most 185 amino acids, harboring four arginine residues, are methylated by CARM1 (Fig. 1B, denoted as construct *d*). This C-terminal portion of TARPP was further subdivided into two fragments of ~100 amino acids each, with construct “*e*” being a good methyl-acceptor and construct “*f*” far less so. The fact that fragment *f* can be methylated *in vitro*, albeit at a low level, may point toward an additional minor methylation site closer to the C-terminal end of TARPP. We concentrated on identifying the major methylation site and subdivided construct “*e*” into two pieces that each harbored just one arginine residue. In this manner the predominant *in vitro* methylated region was mapped to an 80-amino acid stretch that contained a single arginine residue (Arg<sup>650</sup>) (Fig. 1B, construct *g*). Next, we used MEF extracts as a source of methyltransferase activity to transfer a tritium-labeled methyl group from AdoMet onto GST fusion proteins harboring the methylatable motifs of TARPP and PABP1, and the GAR motif of fibrillarin. Cell extracts from *Carm1*<sup>-/-</sup> MEF lines were unable to methylate GST-TARPP or GST-PABP1, but GST-GAR (an *in vitro* substrate for PRMT1, -3 and -6) was methylated by the knock-out lines (Fig. 1C). There is a major methylated band that runs at the gel front. This phenomenon has been seen in other studies (11, 12) and is likely because of degraded recombinant protein that acts as a good substrate. These *in vitro* data identify the region of arginine methylation in the TARPP molecule and suggest that methylation of TARPP by CARM1 is a non-redundant process.

**Full-length TARPP Is Methylated in Vivo**—To determine whether TARPP is methylated in cells we used an *in vivo* methylation assay described by Liu and Dreyfuss (21). The total methylated protein pool is labeled by incubating cells with L-[methyl-<sup>3</sup>H]methionine in the presence of the protein synthesis inhibitor, cycloheximide. HeLa cells were transiently transfected with GFP, GFP-TARPP, and GFP-PABP1 and the methylated proteins labeled as described under “Experimental Procedures.” GFP-PABP1 serves as a positive control for *in vivo* methylation (16). GFP is a negative control to confirm that translation was indeed inhibited. Both the GFP fusions of TARPP and PABP1 are methylated in HeLa cells, whereas GFP alone remains largely unmodified (Fig. 2A), indicating that cellular TARPP (fused to GFP) is methylated. Next, the single arginine residue that was identified as the *in vitro* methylation site (Fig. 1B) was replaced with an alanine residue to generate GFP-TARPP<sup>A650</sup>. HeLa cells were transiently transfected with GFP-TARPP and GFP-TARPP<sup>A650</sup> and the methylated proteins labeled. After immunoprecipitation with  $\alpha$ GFP antibodies it was clear that the GFP fusion of TARPP but not

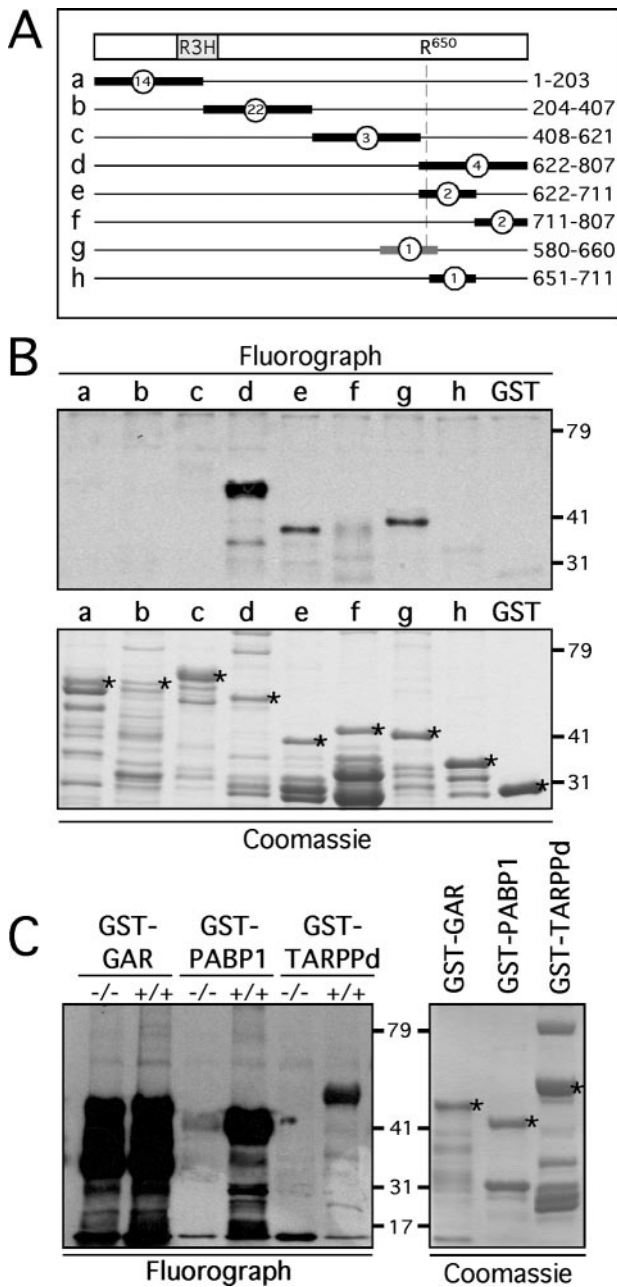


**FIG. 1. Deletion analysis of TARPP identifies the arginine-methylated region.** *A*, diagram of the regions of TARPP that were fused to GST for deletion analysis. The number of arginine residues within each fragment is indicated in a circle. *B*, purified GST fusion proteins were incubated with recombinant CARM1 in the presence of [<sup>3</sup>H]AdoMet and separated by SDS-PAGE. The methylated proteins were visualized by fluorography (exposure time, 18 h) (upper panel). For quantification purposes, the set of methylation substrates was separated by SDS-PAGE and stained with Coomassie (lower panel). As varying degrees of premature termination or degradation of the GST-fused substrates is seen, an asterisk indicates the expected size of each full-length fusion protein. *C*, GST-TARPPd cannot be methylated when using CARM1 knock-out cell extracts as an enzyme source. A wild type MEF extract, but not an extract from a CARM1 knock-out line, was able to methylate the recombinant CARM1 substrates GST-PABP1 and GST-TARPPd. Both CARM1 knock-out and wild type cell line extracts methylated the PRMT1 substrate GST-GAR (left panel). For quantification purposes the set of methylation substrates was separated by SDS-PAGE and stained with Coomassie (right panel). The asterisk indicates the expected size of the full-length fusion protein.

TARPP<sup>A650</sup> was methylated in HeLa cells (Fig. 2*B*), demonstrating that arginine 650 is the only methylated residue in TARPP. In a number of studies arginine methylation has been

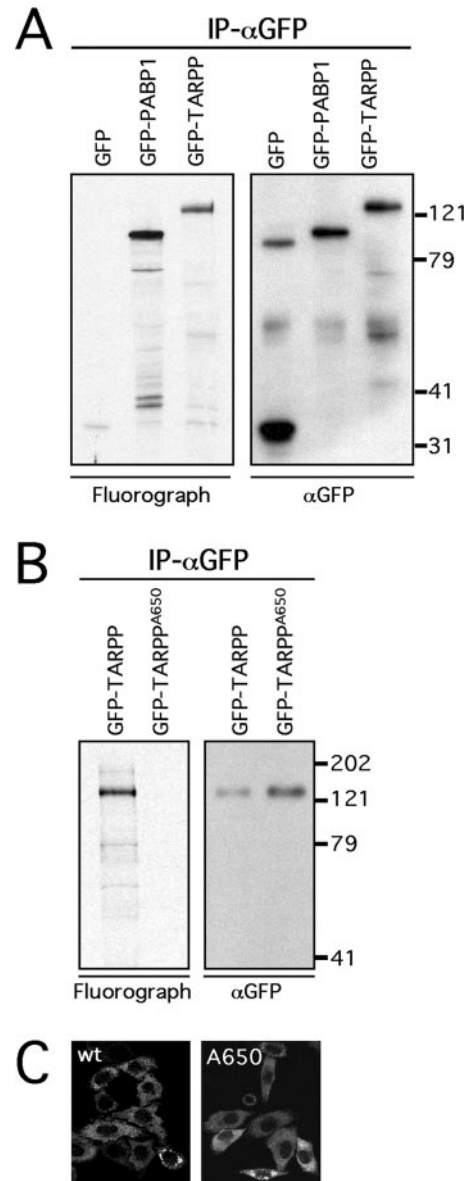


**FIG. 2. TARPP is methylated *in vivo*.** *A*, the GFP fusion protein of TARPP is methylated *in vivo*. HeLa cells were transiently transfected with GFP, GFP-PABP1, and GFP-TARPP. Methylated proteins were labeled *in vivo*. Immunoprecipitations (IP) were performed with αGFP antibodies. The <sup>3</sup>H-labeled proteins were visualized by fluorography (left panel) (exposure time, 5 days), and the same membrane was subsequently immunoblotted with an αGFP antibody (right panel). *B*, arginine 650 is the site of TARPP methylation *in vivo*. HeLa cells were transiently transfected with GFP-TARPP and GFP-TARPP<sup>A650</sup>. Methylated proteins were labeled *in vivo*. Immunoprecipitations were performed with an αGFP antibody. The <sup>3</sup>H-labeled proteins were visualized by fluorography (left panel) (exposure time, 3 days), and the same membrane was immunoblotted with an αGFP antibody (right panel). *C*, the subcellular localization of GFP-TARPP<sup>A650</sup> is not altered. HeLa cells were transiently transfected with GFP-TARPP and GFP-TARPP<sup>A650</sup>. Confocal images were captured.

implicated in the regulation of protein subcellular localization (24). We thus compared the localization of GFP-TARPP and GFP-TARPP<sup>A650</sup>. Even though GFP-TARPP<sup>A650</sup> cannot be methylated in the cell (Fig. 2*B*), no effect on its subcellular localization was observed (Fig. 2*C*).

**TARPP Is Methylated in Immature T Cells**—TARPP expression is restricted to the brain and immature T cells (20). We have demonstrated that ectopically expressed TARPP is methylated in HeLa cells (Fig. 2*A*) and that the site of methylation is Arg<sup>650</sup> (Fig. 2*B*). To study endogenous TARPP we generated

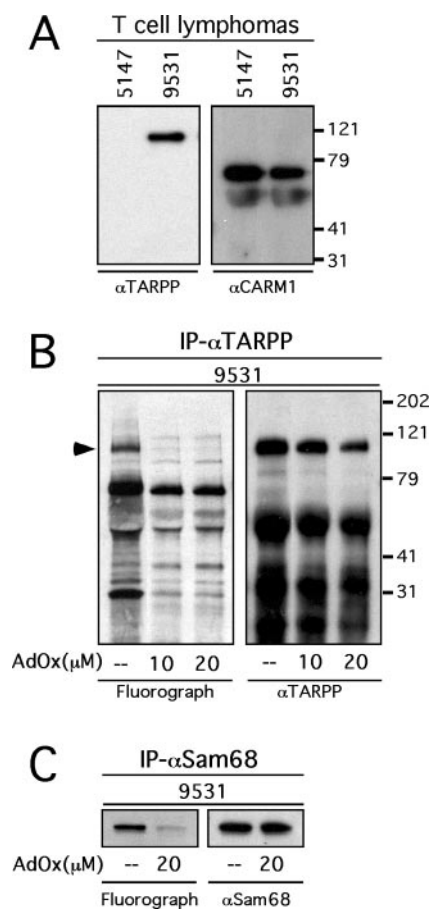


**FIG. 3. Endogenous TARPP is arginine-methylated in immature T cells.** *A*, an immature T cell line expresses both TARPP and CARM1. Protein was extracted from mature (BW5147) and immature (LR1-9531) T cell lines and subjected to Western blot analysis with  $\alpha$ TARPP (left panel) and  $\alpha$ CARM1 (right panel) antibodies. *B*, TARPP is methylated in the immature (LR1-9531) T cell line. Methylated proteins were labeled *in vivo*. Immunoprecipitations were performed with an  $\alpha$ TARPP antibody. The  $^3\text{H}$ -labeled proteins were visualized by fluorography (left panel) (exposure time, 30 days), and the same membrane was immunoblotted with an  $\alpha$ TARPP antibody (right panel). In the presence of 10 and 20  $\mu\text{M}$  adenosine dialdehyde, a global methylation inhibitor, methylation of endogenous TARPP is lost. *C*, methylation of endogenous Sam68 in the immature T cell line. Under the same conditions as depicted in panel *B*, Sam68 methylation in T cells is inhibited with 20  $\mu\text{M}$  adenosine dialdehyde. Fluorographic exposure time, 24 h.

polyclonal antibodies to the human protein. TARPP expression was detected in a T cell line (LR1-9531) derived from an *atm*<sup>-/-</sup>*rag-2*<sup>-/-</sup> thymoma that displays an immature T cell phenotype (22) (Fig. 3A). TARPP expression was not detected in the mature T cell line BW5147. Both mature and immature T cell lines express CARM1. To establish that endogenous TARPP is methylated, an *in vivo* methylation assay was performed on the T cells by incubating them with L-[methyl-<sup>3</sup>H]methionine in the presence of cycloheximide. TARPP was immunoprecipitated from these labeled cell extracts. TARPP was methylated in the immature T cell line (9531), and this methylation was inhibited in the presence of the global methylation inhibitor, adenosine dialdehyde (Fig. 3B). The arrowhead indicates the position of TARPP. Similar results were obtained when a known arginine-methylated protein, Sam68, was subjected to the same analysis (Fig. 3C). The presence of nonspecific bands seen in the TARPP fluorography may be because of the long exposure time (30 days) needed to clearly see the methylation of endogenous TARPP. This long exposure time is needed because only a single site (Arg<sup>650</sup>) on TARPP is

methylated, as opposed to multiple arginine methylation sites in Sam68 (18) and PABP1 (16). Thus, during its brief period of expression in immature T cells, TARPP is likely methylated specifically by CARM1.

**CARM1 Knock-out Mice Exhibit Aberrant T Cell Development**—TARPP is expressed in thymocyte progenitors (20) and is methylated by CARM1 (16) (Figs. 1–3). These results, together with the smaller thymi observed in sections of *Carm1*<sup>-/-</sup> embryos (data not shown), prompted us to investigate T cell development in the *Carm1* mutant embryos. T cell maturation is a highly ordered process in which discrete developmental stages are defined by cell surface expression of well defined differentiation markers such as the coreceptor molecules CD4 and CD8 (reviewed in Refs. 25–27). The earliest intrathymic progenitors, which have a CD4<sup>-</sup>CD8<sup>-</sup>DN phenotype, give rise to the predominant cortical CD4<sup>+</sup>CD8<sup>+</sup> double positive subset. Double positive thymocytes that express  $\alpha\beta$  T cell receptors (TCRs) with appropriate affinity for endogenous peptide/major histocompatibility complexes undergo positive selection during which either CD4 or CD8 is down-regulated. The resulting single positive thymocytes migrate to the medulla, undergo further maturation, and emigrate as naive T cells to peripheral lymphoid tissues (reviewed in Refs. 28, 29). Thymocyte cellularity is greatly reduced in E18.5 *Carm1*<sup>-/-</sup> embryos compared with wild type littermates (Fig. 4A). Flow cytometric analysis showed a decrease in the percentage of DN thymocytes in *Carm1*<sup>-/-</sup> (8%) compared with wild type (22%) thymi (Fig. 4D). Although there is a corresponding increase in the percentage of DP thymocytes in homozygous *Carm1*<sup>-/-</sup> mice, the total number of thymocytes in each major subset is reduced (Fig. 4, B and C).

These findings suggested that CARM1 affects the differentiation and/or survival of T cell precursors. To explore this possibility, we evaluated DN thymocyte maturation in greater detail. Subsets within the DN population can be recognized by the pattern of CD44 and CD25 expression (30). The CD44<sup>+</sup>CD25<sup>-</sup>DN1 subset contains multipotent progenitors that are not yet committed to the T cell lineage (31, 32). Rearrangement of the TCR  $\beta$ -chain locus is initiated at the CD44<sup>+</sup>CD25<sup>+</sup>DN2 stage and continues as thymocytes advance to the CD44<sup>-</sup>CD25<sup>+</sup>DN3 stage. DN3 thymocytes are committed to the T lineage but cannot differentiate to the CD44<sup>-</sup>CD25<sup>-</sup>DN4 stage unless they express pre-TCR heterodimers that consist of a TCR  $\beta$ -chain associated with an invariant pre-TCR $\alpha$  polypeptide. Pre-TCR signaling results in CD25 down-regulation, multiple rounds of proliferation, CD4 and CD8 expression, allelic exclusion at the TCR  $\beta$ -chain locus, and initiation of TCR  $\alpha$ -chain gene rearrangement (reviewed in Ref. 33). Interestingly, Fig. 4E shows an increased proportion of DN1 thymocytes in *Carm1*<sup>-/-</sup> mice. Thus, the absence of CARM1 results in a partial arrest of thymocyte maturation at an early progenitor stage. Because of the developmental block at the DN1 stage, there is a notable reduction in the frequency and absolute number of DN2 thymocytes in *Carm1*<sup>-/-</sup> compared with wild type mice. Nevertheless, the small numbers of DN2 thymocytes that escape or bypass the developmental block imposed by a deficiency in CARM1 retain the ability to undergo developmental progression to DN3 and DN4 stages. Because it has been shown that the DN2 subset contains a high frequency of proliferating cells (34), it is not surprising that the minor DN2 subset in *Carm1*<sup>-/-</sup> mice generates readily detectable DN3 cells, which are the immediate precursors of the DN4 thymocytes. DN4 thymocytes then undergo further expansion to generate the double positive subset (34). However, because of the developmental block at the DN1 progenitor stage in *Carm1*<sup>-/-</sup> mice, there is a severe reduction in the absolute

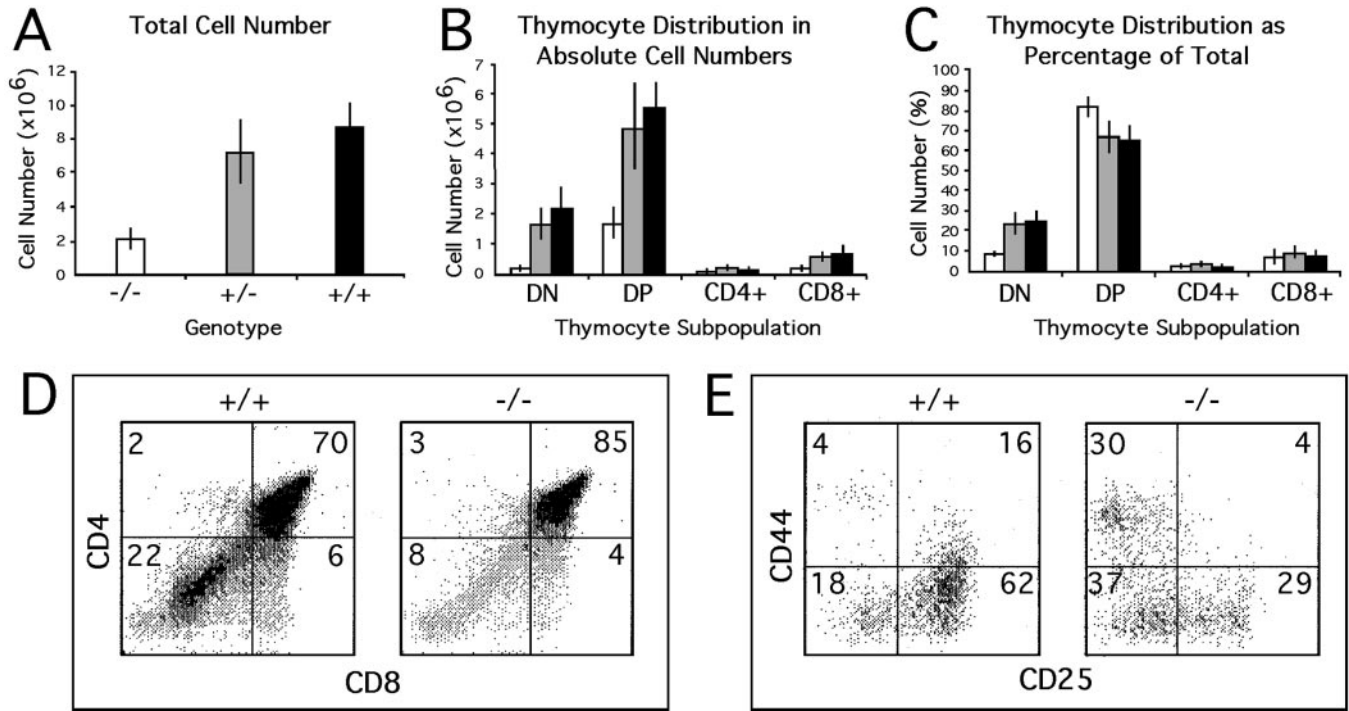


**FIG. 4. Embryos that are null for CARM1 display aberrant T cell development.** Graphic representation of thymocyte cellularity (A) and thymocyte subset distribution (B and C). Thymocytes from E18.5 embryos were counted prior to immunofluorescence staining and flow cytometric analysis for the expression of differentiation markers. Three litters of embryos were analyzed comprising +/+ ( $n = 6$ ), ± ( $n = 11$ ), and -/- ( $n = 5$ ). The S.D. for each group is shown. Flow cytometric analysis of thymocytes from wild type cells (+/+ panels) and CARM1 mutant (-/- panels) mice for the expression of CD4 versus CD8 in the total thymocyte population (D) and CD44 versus CD25 in the gated DN compartment (E). The percentage of cells in each quadrant is depicted in the upper corners.

number of thymocytes at subsequent maturation stages, an effect that accounts for the overall reduction in thymocyte cellularity that occurs in the absence of CARM1 expression. Finally, the results demonstrate that CARM1 plays a role in the differentiation of early thymocyte progenitors. The block at the DN1 to DN2 transition is consistent with the fact that TARPP expression is initiated at the DN2 stage in wild type thymocytes (20).

Here we have presented the following evidence that TARPP is methylated predominantly at one arginine residue by CARM1: 1) TARPP was identified in an *in vitro* screen as a specific substrate for recombinant CARM1 (7); 2) the *in vitro* methylation of TARPP was mapped to arginine 650 within the C-terminal portion of the molecule (Fig. 1B); 3) TARPP is not methylated when using a cell extract from CARM1 knock-out cells as the enzyme source (Fig. 1C), thus providing genetic proof that CARM1 is the enzyme that is modifying TARPP; and 4) a GFP-TARPP fusion that has arginine 650 replaced with an alanine is not methylated *in vivo* (Fig. 2B). Thus within the context of the full-length TARPP the replacement of a single arginine residue prevents *in vivo* methylation. The fact that TARPP expression is largely restricted to thymocyte progenitors led us to compare T cell development in CARM1 wild type and knock-out embryos.

The T cell developmental block in *Carm1*<sup>-/-</sup> mice at the CD44<sup>+</sup>CD25<sup>-</sup> stage may be caused by the lack of TARPP arginine methylation at the CD44<sup>+</sup>CD25<sup>+</sup> stage. The biological function of TARPP is unknown. However, it is intriguing that TARPP expression accompanies TCR gene rearrangement and that TARPP harbors a R3H domain that is likely involved in nucleic acid binding (35). Many CARM1 substrates possess nucleic acid binding properties (PABP1, Hu antigen R, SmB, and histone H3), but others can remodel chromatin (p300/CBP). CARM1 is a positive regulator of p300/CBP function (6, 7), and it may be this co-activator property of CARM1 that,

when lost, results in reduced TCR gene rearrangement because of diminished accessibility to the recombination machinery. Indeed, there is a strong correlation between hyperacetylated and accessible regions of TCR loci *in vivo* (36). Thus, lysine acetylation and arginine methylation may work together to enhance chromatin accessibility for RAG-mediated cleavage in the same way that these modifications synergize for nuclear receptor-regulated transcription (37). Finally, it is possible that the absence of CARM1 indirectly affects thymocyte development by impairing the function of non-lymphoid cells that comprise the thymic microenvironment. In particular, thymocyte differentiation and survival are dependent on signals emanating from the thymic epithelial compartment (26). Therefore, future studies will dissect the significance of CARM1 expression in thymocytes versus thymic stromal cells.

REFERENCES

1. Bedford, M. T., Frankel, A., Yaffe, M. B., Clarke, S., Leder, P., and Richard, S. (2000) *J. Biol. Chem.* **275**, 16030–16036
2. Friesen, W. J., Massenot, S., Paushkin, S., Wyce, A., and Dreyfuss, G. (2001) *Mol. Cell* **7**, 1111–1117
3. Gary, J. D., and Clarke, S. (1998) *Prog. Nucleic Acids Res. Mol. Biol.* **61**, 65–131
4. Chen, D., Ma, H., Hong, H., Koh, S. S., Huang, S. M., Schurter, B. T., Aswad, D. W., and Stallecup, M. R. (1999) *Science* **284**, 2174–2177
5. Schurter, B. T., Koh, S. S., Chen, D., Bunick, G. J., Harp, J. M., Hanson, B. L., Henschen-Edman, A., Mackay, D. R., Stallecup, M. R., and Aswad, D. W. (2001) *Biochemistry* **40**, 5747–5756
6. Xu, W., Chen, H., Du, K., Asahara, H., Tini, M., Emerson, B. M., Montminy, M., and Evans, R. M. (2001) *Science* **294**, 2507–2511
7. Chevillard-Briet, M., Trouche, D., and Vandel, L. (2002) *EMBO J.* **21**, 5457–5466
8. Henry, M. F., and Silver, P. A. (1996) *Mol. Cell. Biol.* **16**, 3668–3678
9. Gary, J. D., Lin, W. J., Yang, M. C., Herschman, H. R., and Clarke, S. (1996) *J. Biol. Chem.* **271**, 12585–12594
10. Lin, W. J., Gary, J. D., Yang, M. C., Clarke, S., and Herschman, H. R. (1996) *J. Biol. Chem.* **271**, 15034–15044
11. Scott, H. S., Antonarakis, S. E., Lalioti, M. D., Rossier, C., Silver, P. A., and Henry, M. F. (1998) *Genomics* **48**, 330–340
12. Tang, J., Gary, J. D., Clarke, S., and Herschman, H. R. (1998) *J. Biol. Chem.* **273**, 16935–16945
13. Frankel, A., Yadav, N., Lee, J., Branscombe, T. L., Clarke, S., and Bedford,

- M. T. (2002) *J. Biol. Chem.* **277**, 3537–3543
14. Branscombe, T. L., Frankel, A., Lee, J. H., Cook, J. R., Yang, Z., Pestka, S., and Clarke, S. (2001) *J. Biol. Chem.* **276**, 32971–32976
15. Pollack, B. P., Kotenko, S. V., He, W., Izotova, L. S., Barnoski, B. L., and Pestka, S. (1999) *J. Biol. Chem.* **274**, 31531–31542
16. Lee, J., and Bedford, M. T. (2002) *EMBO Rep.* **3**, 268–273
17. Yadav, N., Lee, J., Kim, J., Shen, J., Hu, M. C., Aldaz, C. M., and Bedford, M. T. (2003) *Proc. Natl. Acad. Sci. U. S. A.* **100**, 6464–6468
18. Cote, J., Boisvert, F. M., Boulanger, M. C., Bedford, M. T., and Richard, S. (2003) *Mol. Biol. Cell* **14**, 274–287
19. Li, H., Park, S., Kilburn, B., Jelinek, M. A., Henschen-Edman, A., Aswad, D. W., Stallcup, M. R., and Laird-Offringa, I. A. (2002) *J. Biol. Chem.* **277**, 44623–44630
20. Kisielow, J., Nairn, A. C., and Karjalainen, K. (2001) *Eur. J. Immunol.* **31**, 1141–1149
21. Liu, Q., and Dreyfuss, G. (1995) *Mol. Cell. Biol.* **15**, 2800–2808
22. Reizis, B., and Leder, P. (1999) *J. Exp. Med.* **189**, 1669–1678
23. Bussow, K., Cahill, D., Nietfeld, W., Bancroft, D., Scherzinger, E., Lehrach, H., and Walter, G. (1998) *Nucleic Acids Res.* **26**, 5007–5008
24. McBride, A. E., and Silver, P. A. (2001) *Cell* **106**, 5–8
25. Rodewald, H.-R., and Fehling, H. J. (1998) *Adv. Immunol.* **69**, 1–112
26. Anderson, G., and Jenkinson, E. J. (2001) *Nature Rev. Immunol.* **1**, 31–40
27. Gill, J., Malin, M., Sutherland, J., Gray, D., Hollander, G., and Boyd, R. (2003) *Immunol. Rev.* **195**, 28–50
28. Sebзда, E., Mariathasan, S., Ohteki, T., Jones, R., Bachmann, M. F., and Ohashi, P. S. (1999) *Annu. Rev. Immunol.* **17**, 829–874
29. Jameson, S. C., Hogquist, K. A., and Bevan, M. J. (1996) *Ann. Rev. Immunol.* **13**, 93–126
30. Godfrey, D. I., Kennedy, J., Suda, T., and Zlotnik, A. (1993) *J. Immunol.* **150**, 4244–4252
31. Zuniga-Pflucker, J. C., and Lenardo, M. J. (1996) *Curr. Opin. Immunol.* **8**, 215–224
32. Shortman, K., and Wu, L. (1996) *Annu. Rev. Immunol.* **14**, 29–47
33. Michie, A. M., and Zuniga-Pflucker, J. C. (2002) *Semin. Immunol.* **14**, 311–323
34. Penit, C., Lucas, B., and Vasseur, F. (1995) *J. Immunol.* **154**, 5103–5113
35. Grishin, N. V. (1998) *Trends Biochem. Sci.* **23**, 329–330
36. McMurry, M. T., and Krangel, M. S. (2000) *Science* **287**, 495–498
37. Lee, Y. H., Koh, S. S., Zhang, X., Cheng, X., and Stallcup, M. R. (2002) *Mol. Cell. Biol.* **22**, 3621–3632